



American Society of Hematology
 2021 L Street NW, Suite 900,
 Washington, DC 20036
 Phone: 202-776-0544 | Fax 202-776-0545
 editorial@hematology.org

Ceramide-induced integrated stress response overcomes Bcl-2 inhibitor resistance in acute myeloid leukemia

Tracking no: BLD-2021-013277R2

Alexander Lewis (University of South Australia and SA Pathology, Australia) Victoria Pope (University of South Australia and SA Pathology, Australia) Melinda Tea (University of South Australia and SA Pathology, Australia) Manjun Li (University of South Australia and SA Pathology, Australia) Gus Nwosu (University of South Australia and SA Pathology, Australia) Thao Nguyen (University of Adelaide, Australia) Craig Wallington-Beddoe (University of South Australia and SA Pathology, Australia) Paul Moretti (University of South Australia and SA Pathology, Australia) Dovile Anderson (Monash University, Australia) Darren Creek (Monash University, Australia) Maurizio Costabile (University of South Australia, Australia) Saira Ali (University of South Australia and SA Pathology, Australia) Chloe Thompson-Peach (South Australian Health and Medical Research Institute (SAHMRI), Australia) B Dredge (University of South Australia and SA Pathology, Australia) Andrew Bert (University of South Australia and SA Pathology, Australia) Gregory Goodall (Department of Medicine, University of Adelaide, Australia) Paul Ekert (Peter MacCallum Cancer Centre, Melbourne, Victoria, Australia, Australia) Anna Brown (University of Adelaide, Australia) Richard D'Andrea (University of South Australia, Australia) Nirmal Robinson (University of South Australia and SA Pathology, Australia) Melissa Pitman (University of South Australia and SA Pathology, Australia) Daniel Thomas (Stanford University, United States) David Ross (University of South Australia and SA Pathology, Australia) Briony Gliddon (University of South Australia and SA Pathology, Australia) Jason Powell (University of South Australia and SA Pathology, Australia) Stuart Pitson (University of Adelaide, Australia)

Abstract:

Inducing cell death by the sphingolipid ceramide is a potential anti-cancer strategy, but the underlying mechanisms remain poorly defined. Here, we show that triggering accumulation of ceramide in acute myeloid leukaemia (AML) cells by inhibition of sphingosine kinase induces an apoptotic integrated stress response (ISR) through protein kinase R-mediated activation of the master transcription factor ATF4. This leads to transcription of the BH3-only protein, Noxa, and degradation of the pro-survival Mcl-1 protein on which AML cells are highly dependent on for survival. Targeting this novel ISR pathway in combination with the Bcl-2 inhibitor venetoclax synergistically killed primary AML blasts, including those with venetoclax-resistant mutations, as well as immunophenotypic leukemic stem cells, and reduced leukemic engraftment in patient-derived AML xenografts. Collectively, these findings provide mechanistic insight into the anti-cancer effects of ceramide and pre-clinical evidence for new approaches to augment Bcl-2 inhibition in the therapy of AML and other cancers with high Mcl-1 dependency.

Conflict of interest: No COI declared

COI notes:

Preprint server: No;

Author contributions and disclosures: ACL, MNT, GON, VSP, TMN, CWB, PABM, DA, DJC, MRP, BLG and JAP performed experiments. PGE provided intellectual input and reagents. DMR, ALB and RJD provided patient material and clinical notes. ACL, JAP, DT and SMP designed the studies and analysed the data. ACL, JAP and SMP wrote the manuscript, which all authors critically reviewed and edited.

Non-author contributions and disclosures: No;

Agreement to Share Publication-Related Data and Data Sharing Statement: emails to the corresponding author

Clinical trial registration information (if any):

1 **Ceramide-induced integrated stress response overcomes Bcl-2 inhibitor**
2 **resistance in acute myeloid leukemia**

3 **Running Title:** Ceramide and the integrated stress response in AML

4 **Alexander C. Lewis^{1,#}, Victoria S. Pope¹, Melinda N. Tea¹, Manjun Li¹, Gus O. Nwosu¹, Thao M.**
5 **Nguyen^{1,2}, Craig T. Wallington-Beddoe^{1,2,3,4}, Paul A. B. Moretti¹, Dovile Anderson⁵, Darren J.**
6 **Creek⁵, Maurizio Costabile^{1,6}, Saira R. Ali¹, Chloe A. L. Thompson-Peach^{2,7}, B. Kate Dredge¹,**
7 **Andrew G. Bert¹, Gregory J. Goodall¹, Paul G. Ekert^{8,9,10}, Anna L. Brown^{1,2,11}, Richard**
8 **D'Andrea¹, Nirmal Robinson¹, Melissa R. Pitman^{1,12}, Daniel Thomas^{2,7,13}, David M. Ross^{1,2,3,4,7,14},**
9 **Briony L. Gliddon¹, Jason A. Powell^{1,2,15,*}, Stuart M. Pitson^{1,2,12,15,*}**

10 ¹ Centre for Cancer Biology, University of South Australia and SA Pathology, Bradley Building,
11 North Terrace, Adelaide, SA 5001, Australia

12 ² Adelaide Medical School, Faculty of Health Sciences, University of Adelaide, Adelaide SA, 5000,
13 Australia

14 ³ College of Medicine and Public Health, Flinders University, Bedford Park SA, 5042, Australia

15 ⁴ Flinders Medical Centre, Bedford Park SA, 5042, Australia

16 ⁵ Drug Delivery, Disposition and Dynamics, Monash Institute of Pharmaceutical Sciences, Monash
17 University, Parkville, Victoria, Australia

18 ⁶ Clinical and Health Sciences, University of South Australia, Adelaide, SA 5001, Australia

19 ⁷ Precision Medicine Theme, South Australian Health and Medical Research Institute, Adelaide,
20 Australia

21 ⁸ Children's Cancer Institute, Lowy Cancer Research Centre, University of New South Wales, Sydney,
22 NSW, Australia.

23 ⁹ Peter MacCallum Cancer Centre, Melbourne, Victoria, Australia

24 ¹⁰ Murdoch Children's Research Institute, Royal Children's Hospital, Parkville, Victoria, Australia

25 ¹¹ Department of Genetics and Molecular Pathology, SA pathology, Adelaide, Australia

26 ¹² School of Biological Sciences, University of Adelaide, Adelaide SA, 5000, Australia

27 ¹³ Institute for Stem Cell Biology and Regenerative Medicine, Stanford School of Medicine, Stanford
28 University, Stanford, CA

29 ¹⁴ Department of Haematology and Bone Marrow Transplantation, Royal Adelaide Hospital,
30 Adelaide, Australia.

31 ¹⁵ Equal senior author

32 #Present Address: The Peter MacCallum Cancer Centre, Melbourne, 3000 VIC, Australia.

33 * **Authors for correspondence:** Stuart M Pitson, Bradley Building, North Tce, Adelaide, SA 5001,
34 Australia, E-mail: stuart.pitson@unisa.edu.au, Tel: +61 8 8302 7832. Jason A Powell, Bradley
35 Building, North Tce, Adelaide, SA 5001, Australia, E-mail: jason.powell@sa.gov.au, Tel: +61 8 8302
36 7898.

37 Text word count 3,990, abstract word count 151, 7 figures, 68 references

38 Scientific category: Myeloid Neoplasia

39

40

41 ***Key points***

- 42 • Enhancing cellular ceramide levels in AML activates protein kinase R to induce the integrated
43 stress response (ISR).
- 44 • This ISR induces the BH3-only protein Noxa, resulting in degradation of Mcl-1 and sensitization
45 of AML to Bcl-2 inhibition.

46

47

48 ***Abstract***

49 Inducing cell death by the sphingolipid ceramide is a potential anti-cancer strategy, but the underlying
50 mechanisms remain poorly defined. Here, we show that triggering accumulation of ceramide in acute
51 myeloid leukaemia (AML) cells by inhibition of sphingosine kinase induces an apoptotic integrated
52 stress response (ISR) through protein kinase R-mediated activation of the master transcription factor
53 ATF4. This leads to transcription of the BH3-only protein, Noxa, and degradation of the pro-survival
54 Mcl-1 protein on which AML cells are highly dependent on for survival. Targeting this novel ISR
55 pathway in combination with the Bcl-2 inhibitor venetoclax synergistically killed primary AML
56 blasts, including those with venetoclax-resistant mutations, as well as immunophenotypic leukemic
57 stem cells, and reduced leukemic engraftment in patient-derived AML xenografts. Collectively, these
58 findings provide mechanistic insight into the anti-cancer effects of ceramide and pre-clinical evidence
59 for new approaches to augment Bcl-2 inhibition in the therapy of AML and other cancers with high
60 Mcl-1 dependency.

61

62 **Introduction**

63 The discovery of novel signaling mechanisms that enable induction of pro-apoptotic BH3-only
64 proteins independent of TP53 has immense therapeutic potential for both TP53 mutant cancer and
65 tumors resistant to Bcl-2 inhibitors. Pro-apoptotic Noxa is a Bcl-2 family protein that belongs to a
66 subclass of BH3-only proteins and can induce apoptosis via both TP53-dependent and TP53-
67 independent processes, depending on cellular context. Certain cytotoxic drugs have been shown to
68 upregulate Noxa protein, principally through upregulating mRNA transcription,¹ but the upstream
69 signals and physiological stimuli are not well defined nor are they optimised for therapy. Through its
70 ability to bind and neutralise both A1 and Mcl-1 pro-survival proteins, upregulation of Noxa² has
71 therapeutic potential in multiple cancers that show intrinsic or acquired resistance to Bcl-2 inhibitor
72 therapies such as venetoclax.

73 The BH3 mimetic, venetoclax is a highly selective oral inhibitor of the pro-survival protein
74 Bcl-2 approved for treatment of 17p(del) chronic lymphocytic leukemia.³ Venetoclax shows modest
75 activity as a single agent in AML (overall response rate 19%)⁴ but promising results when combined
76 with chemotherapy (complete response CR, 62%) or hypomethylating agents (CR 67%),^{5,6} and has
77 been recently approved by the FDA in adults 75 years or older, or who have comorbidities precluding
78 intensive induction chemotherapy (NCT02993523 and NCT03069352). Unlike lymphoid leukemias,
79 AML cells rely on the pro-survival protein Mcl-1 for disease maintenance,⁷ suggesting that its
80 inhibition may prove beneficial in achieving deep molecular remission. Pre-clinical studies revealed
81 Mcl-1 as a biomarker for venetoclax resistance due to the inability of this drug to sequester Mcl-1,
82 highlighting the importance of concurrent inhibition of multiple proteins in the Bcl-2 family.^{4,8}

83 An alternative mechanism for induction of programmed cell death can occur through the
84 ceramide/sphingosine-1-phosphate (S1P) rheostat.⁹ Ceramide accumulation is thought to contribute to
85 the effects of many anti-cancer therapies including ionizing radiation, daunorubicin, etoposide and
86 gemcitabine as well as some targeted therapies such as tyrosine kinase inhibitors.¹⁰ Ceramides are
87 lipids present in high concentrations in cell membranes, but accumulate following blockade of
88 downstream conversion of sphingosine to S1P, that occurs principally through the activity of
89 sphingosine kinase 1 (SPHK1). SPHK1 can promote tumorigenic pathways such as survival and

90 proliferation in multiple solid and blood cancers, and is a key player of the sphingolipid rheostat in
91 maintaining the balance between pro-apoptotic ceramide and sphingosine and pro-survival S1P.¹¹ But,
92 how sphingolipid signaling is integrated with intrinsic BAX/BAK-dependent apoptosis is not well
93 understood.

94 We previously demonstrated that targeting SPHK1 in AML depletes the pro-survival protein,
95 Mcl-1 and can synergise with Bcl-2/Bcl-X_L inhibitor, navitoclax.¹² However, the mechanistic basis of
96 synergy between SPHK1 inhibition and navitoclax remained poorly defined. Here, we show that
97 triggering accumulation of ceramide in AML cells by inhibition of SPHK1 induces upregulation of
98 the BH3-only protein Noxa via ceramide-mediated activation of protein kinase R (PKR), as part of the
99 integrated stress response (ISR) pathway, and subsequent activation of the transcription factor ATF4.
100 Targeting this novel pathway synergizes with the clinically relevant Bcl-2 inhibitor, venetoclax to
101 exert anti-leukemic activity against AML patient blasts, including those harboring mutations
102 associated with venetoclax resistance and immunophenotypic CD34⁺CD38⁻CD123⁺ leukemic stem
103 cells (iLSCs), both in vitro and in vivo. Collectively this advocates the use of ceramide modulating
104 agents as ISR activators to augment Bcl-2 inhibiting strategies for the treatment of AML and other
105 cancers with high dependency on Mcl-1.

106

107 *Methods*

108 *Study approval*

109 Animal studies were approved by the SA Pathology/CALHN and UniSA Animal Ethics Committees.
110 Human samples were obtained from the South Australian Cancer Research Biobank from AML
111 patients after informed consent, and studies were approved by the Royal Adelaide Hospital Human
112 Ethics Committee (Protocol # 041009).

113 *Mutational analysis of primary AML biopsies*

114 Mutations in primary AML biopsies were identified using either whole exome sequencing or targeted
115 gene sequencing as described previously.¹²

116 *Cell lines & primary AML samples*

117 AML cell lines MV411, THP-1, MOLM13 and UT7 were cultured as previously described.¹² OCI-
118 AML3 were cultured in RPMI with 10% fetal calf serum (FCS; HyClone Thermo Scientific), HL-60
119 in IMDM with 20% FCS, and HEK293T cells in DMEM with 10% FCS. Cell line authentication was
120 confirmed by STR profiling. Mononuclear cells (MNC) from diagnostic bone marrow or apheresis
121 product samples were isolated by Ficoll-Hypaque density-gradient centrifugation and resuspended in
122 IMDM containing 10% FCS. Factor dependent myeloid (FDM) wild type and $Bax^{-/-}/Bak^{-/-}$ cells were
123 cultured in DMEM (Low glucose) supplemented with 10% FCS and 0.25ng/ml mL-3. Parental and
124 PERK^{-/-} HAP1 cells (Horizon Discovery) were cultured in IMDM containing 10% FCS.

125 *In vivo primary AML xenograft model*

126 6 week old female NOD/SCID/IL-2R $\gamma^{-/-}$ (NSG) mice were IV injected with 5×10^6 human primary
127 AML cells. Mice were tail bled weekly to confirm human cell engraftment by flow cytometry (>1%
128 hCD45+). MP-A08 (100mg/kg i.p. {PEG 400}) and venetoclax (75mg/kg p.o. {60% Phosal 50PG,
129 30% PEG 400 and 10% ethanol}) were administered daily for two weeks. Mice were sacrificed
130 following treatment cessation to collect bone marrow to measure hCD45+ cells by flow cytometry.
131 Immunohistochemistry on mouse sternum was performed as previously described using the human
132 specific mitochondrial antibody (Thermo Fisher Scientific Cat# MA1-21891).¹²

133 Data Sharing Statement: For original data please contact stuart.pitson@unisa.edu.au

134 Additional details are provided in supplemental methods

135

136 **Results**

137 ***BH3-only protein Noxa is essential for AML cell death induced by SPHK1 inhibition***

138 Previous studies have shown that SPHK1 inhibitors, including MP-A08, induce AML cell death.¹²⁻¹⁶
139 We also showed this occurs in an Mcl-1-dependent manner,¹² however, the exact mechanism
140 remained unclear. The BH3-only protein Noxa is a selective binding partner of Mcl-1, with this
141 interaction known to promote Mcl-1 degradation and induction of apoptosis.¹⁷ Treatment of MV411
142 AML cells with the SPHK1 inhibitor MP-A08 increased Noxa expression and augmented the
143 association of Noxa with Mcl-1 (Figure 1a). This increase in Noxa protein expression coincided with

144 increased Noxa mRNA levels following MP-A08 treatment (Figure 1b; Supp Figure 1) and could be
145 blocked through inhibition of protein synthesis by cycloheximide (Figure 1c), suggesting that
146 increased Noxa expression occurs via transcriptional upregulation. Similar increases in Noxa
147 expression were also observed in both MV411 cells and primary AML patient samples (Supp. Table
148 1) in response to another structurally different SPHK1 inhibitor, SK1-I (Supp. Figure 2). A broader
149 analysis of Bcl-2 and BH3-only proteins in response to MP-A08 prior to apoptosis induction (6 h) in
150 multiple AML cell lines revealed dose-dependent increases in Noxa and to a lesser extent other BH3
151 only proteins Bim and cleaved Bid, but not other Bcl-2 family proteins nor TP53 (Figure 1d,e; Supp
152 Figure 3a,b). Doxycycline-inducible shRNA knockdown of Noxa partially reversed the degradation of
153 Mcl-1 and rescued the effects of MP-A08 on cell viability (Figure 1f; Supp Figure 3c). In contrast,
154 Bim knockdown had only a minor effect on cell viability (Figure 1g) but could not reverse loss of
155 Mcl-1, whereas Bid knockdown had no effect (Figure 1h). This implicates Noxa as an important
156 determinant of the apoptotic effects of SPHK1 inhibition in AML cells.

157

158 ***SPHK1 inhibition induces ATF4-dependent Noxa transcription***

159 Tumour suppressor TP53 has been previously shown to directly induce Noxa transcription in response
160 to chemotherapeutics.¹⁸ Unlike daunorubicin and cytarabine, MP-A08 treatment of multiple AML cell
161 lines was associated with a lack of increased TP53 expression, suggesting that the increase in Noxa is
162 independent of TP53 (Figure 2a; Supp Figure 4). Previous work investigating the mechanism of MP-
163 A08-induced AML cell death using Ingenuity Pathways Analysis (IPA) of RNA-Seq data revealed
164 enrichment of genes associated with the unfolded protein response (UPR).¹² In response to cellular
165 stresses that cause misfolded proteins to accumulate within the endoplasmic reticulum (ER), cells
166 activate the three UPR transmembrane proteins, ATF6 (activating transcription factor-6), IRE1
167 (inositol-requiring kinase 1) and protein kinase R-like ER kinase (PERK) to re-establish proteostasis
168 (Figure 2b). Further examination of this RNA-Seq data revealed that MP-A08 treatment of MV411
169 cells induced almost exclusively activation of the PERK arm of the UPR, typified by upregulation of
170 ATF4 and downstream effectors, including CHOP (Supp. Figure 5a).¹² Direct protein analysis of this
171 pathway demonstrated that MP-A08 induced clear activation/phosphorylation of eIF2 α , a central

172 component of the pathway, and induction of ATF4 in AML cell lines (Figure 2c; Supp Figure 5b).
173 Similar effects were also observed with CRISPR/Cas9-mediated knockout of SPHK1 (Figure 2d;
174 Supp. Figure 5c). Intriguingly, consistent with the RNA-Seq data, no changes in XBP1 splicing were
175 observed in response to MP-A08 treatment (Supp. Figure 5d), further demonstrating that the effects
176 induced by SPHK1 inhibition are limited to the PERK arm of the UPR. Notably, prolonged activation
177 of the PERK pathway can culminate in upregulation of BH3-only proteins, Noxa and Bim through the
178 transcription factors ATF4 and CHOP, respectively.^{19,20} To confirm that ATF4 was necessary to
179 mediate Noxa transcription in response to MP-A08, we utilised the eIF2b agonist, ISRIB to render
180 cells insensitive to eIF2a phosphorylation and block ATF4 production²¹ which nullified Noxa
181 transcription observed with MP-A08 treatment (Figure 2e; Supp Figure 1). An ATF4 shRNA
182 recapitulated the effects of ISRIB (Figure 2f; Supp Figure 6). Chromatin immuno-precipitation (ChIP)
183 analysis of the Noxa promoter confirmed the involvement of ATF4 in Noxa transcription with
184 significant enrichment of ATF4 following MP-A08 treatment (Figure 2g). Like observed in AML cell
185 lines, MP-A08 treatment resulted in dose-dependent increases in eIF2a phosphorylation, Noxa
186 expression and ATF4 expression in a series of primary AML patient blasts (Figure 2h).

187

188 *Ceramide accumulation activates an apoptotic integrated stress response*

189 Ceramides have been shown to evoke UPR activation and contribute to disease pathogenesis.²²
190 Furthermore, saturated lipids, of which the ceramides and other sphingolipids are a major class, have
191 been shown to induce IRE1 and PERK activation independent of unfolded proteins via direct sensing
192 of the lipid composition within the ER membrane.²³⁻²⁶ As the ER is the main location of de novo
193 sphingolipid biosynthesis, we hypothesized that the accumulation of sphingolipids, such as ceramides,
194 at this site in response to SPHK1 inhibition may facilitate the PERK activation observed in response
195 to MP-A08. Indeed, mass spectrometric lipidomic analysis of MV411 cells treated with MP-A08 for 6
196 h revealed a broad increase in the cellular levels of various ceramides and dihydroceramides, as well
197 as sphingosine and dihydrosphingosine (Figure 3a-c). Similar MP-A08-induced increases in
198 ceramides, but not dihydroceramides, were also observed in MOLM13 and OCI-AML3 cells, with an
199 apparent bias towards increases in long chain ceramides over very long chain ceramides (Supp Figure

200 7). In MV411 cells increases in ceramides and dihydroceramides were observed as early as 2 h (Supp.
201 Figure 8), in alignment with the upregulation of ATF4 and Noxa observed at this time point after
202 SPHK1 inhibition by MP-A08 (Figure 2c). Consistent with a role for ceramides/dihydroceramides in
203 these effects, use of PF-543, a potent SPHK1 inhibitor that blocks S1P generation but inexplicably
204 does not increase ceramide levels,²⁷ did not induce eIF2a phosphorylation, nor increase ATF4 and
205 Noxa levels, nor reduce Mcl-1 levels (Figure 3d). In contrast, the ceramidase inhibitor, ceranib-2,
206 known to elevate cellular ceramide levels,²⁸ caused induction of Noxa and loss of Mcl-1, as well as
207 effective cell death of AML cell lines (Figure 3e; Supp Figure 9). Together, this data suggests that
208 accumulation of ceramides mediates the anti-AML effects of SPHK1 inhibition, rather than loss of
209 S1P signaling. Indeed, addition of exogenous S1P failed to rescue AML cell death induced by MP-
210 A08 (Supp. Figure 10). To more directly examine the effects of ceramide we added exogenous C2- or
211 C6-ceramide to MV411 cells which, unlike the respective dihydroceramides, induced ATF4 and Noxa
212 expression and loss of Mcl-1, consistent with a role for ceramides in evoking activation of the ATF4
213 pathway (Figure 3f).

214 Since our data demonstrated a clear involvement of eIF2a and ATF4 in mediating the effects
215 of SPHK1 inhibition on Noxa accumulation, we next examined the dependency on PERK through the
216 use of both CRISPR/Cas9 knockout of PERK in HAP1 chronic myeloid leukemia cells and
217 doxycycline-inducible shRNA knockdown of PERK in MV411 cells. Unexpectedly, loss of PERK
218 had no effect on MP-A08-induced ATF4 and Noxa accumulation (Figure 3g,h,i) suggesting this may
219 be driven by an alternative mechanism leading to activation/phosphorylation of eIF2a.

220

221 ***Ceramides drive an integrated stress response via direct activation of PKR***

222 In addition to PERK, eIF2a can be phosphorylated by three other protein kinases that are activated
223 under varying stress conditions as part of the ISR. These kinases, PKR, GCN2 (general control non-
224 derepressible 2) and HRI (heme-regulated inhibitor) can all phosphorylate eIF2a to increase
225 translation of the master ISR transcription factor, ATF4²⁹ (Figure 4a). Pharmacological interrogation
226 of the role of these kinases in ATF4 and Noxa induction revealed a clear role for PKR with two
227 different PKR inhibitors C16³⁰ and 2-aminopurine (2-AP),³¹ both blocking the effects of MP-A08

228 (Figure 4b,c). In contrast, inhibition of GCN2 (with A-92) or PERK (with AMG-44) had little to no
229 effect (Figure 4b). Similar effects were observed in all five AML cell lines examined (Figure 4b,c).
230 Furthermore, the anti-AML effects of MP-A08 on THP-1 and HL-60 cells were mitigated by either
231 pharmacological targeting of PKR with 2-AP (Figure 4d; Supp Figure 11), or CRISPR/Cas9 knockout
232 of PKR in MV411 cells (Figure 4e). Collectively, this indicates a critical role for PKR in sensing
233 SPHK1-inhibitor-induced ceramide accumulation, culminating in activation of eIF2a, leading to
234 activation of ATF4 and Noxa, loss of Mcl-1 and consequent AML cell death.

235 Previous findings that ceramide can directly modulate the function of various proteins,³²⁻³⁷
236 suggested the potential for PKR to be directly activated by ceramide. To examine this we assessed the
237 effect of ceramide on the activity of isolated PKR in vitro. Strikingly, our results demonstrated
238 enhanced PKR activity in the presence of ceramide suggesting that ceramide directly binds and
239 enhances PKR kinase activity (Figure 4f). To further assess the interaction of ceramide with PKR we
240 employed ceramide conjugated agarose beads to probe cell lysates for PKR. The data (Figure 4g)
241 demonstrates a clear pull-down of PKR with ceramide beads compared to control beads, indicative of
242 an interaction of PKR with ceramide.

243

244 *SPHK1 inhibition synergises with venetoclax in AML cell lines*

245 Mcl-1 is known to mediate resistance to Bcl-2 inhibition in AML,⁸ and approaches to target Mcl-1
246 have been shown to enhance the efficacy of Bcl-2 inhibition in inducing AML cell death.^{12,38-42} Thus,
247 we next investigated the therapeutic potential for modulating sphingolipid signaling to impact Bcl-2
248 antagonism. Anti-AML synergy of MP-A08 and venetoclax could be observed as early as two hours
249 (Figure 5a) and coupled with enhanced association of Noxa with Mcl-1 (Supp. Figure 12a,b).

250 Viability studies on factor-dependent myeloid cell lines from wild type and *Bax*^{-/-}/*Bak*^{-/-}
251 mice⁴³ demonstrated that wild type cells underwent synergistic cell death in response to MP-A08 and
252 venetoclax, but *Bax*^{-/-}/*Bak*^{-/-} cells were completely resistant (Figure 5b), verifying mitochondrial
253 mediated apoptosis via the necessity of executioner proteins, Bax and Bak.

254 Combining MP-A08 with sub-cytotoxic doses of venetoclax strongly enhanced cell death in
255 venetoclax-sensitive MV411, HL-60 and MOLM13 cell lines (Figure 5c-f), as well as in the

256 venetoclax-resistant OCI-AML3 cell line (Figure 5g). Statistical analysis using the Chou-Talalay
257 method⁴⁴ confirmed combinational treatment induced synergistic cell death (synergy = combination
258 index (CI) <1). Treatment of MV411 cells with another SPHK1 inhibitor, SK1-I, recapitulated the
259 effects observed with MP-A08, causing synergistic loss of cell viability with venetoclax treatment
260 (Supp. Figure 12c). Synergy between SPHK1 and Bcl-2 inhibition was further confirmed by
261 doxycycline-inducible shRNA targeting of Bcl-2 in MV411 cells (Figure 5h). Interestingly, at doses
262 capable of achieving drug synergy in other cells, MP-A08 and venetoclax treatment exhibited little
263 effect in UT7 cells (Figure 5i). This lack of response to either drug, however, may be explained either
264 by the strong expression of Bcl-X_L (Supp. Figure 12d)⁴⁵ or by the lack of Mcl-1 degradation in
265 response to MP-A08 (Figure 5j). Combined treatment was associated with synergistic activation of
266 caspase 3 and loss of Mcl-1 across several AML cell lines (Figure 5k,l, Supp. Figure 12e).

267

268 ***MP-A08 and venetoclax treatment exhibits anti-leukemic activity in primary AML cells in vitro and***
269 ***in vivo***

270 MP-A08 treatment of primary AML samples induced changes in levels of Mcl-1, Noxa and Bid
271 (Figure 6a). Combining both MP-A08 and venetoclax also resulted in synergistically enhanced cell
272 death of primary AML blasts (Figure 6b-c) and chemo-refractory and relapse driving iLSCs (Figure
273 6d) even when co-cultured with human bone marrow derived mesenchymal stem cells (MSC) (Figure
274 6e; Supp. Figure 13a). This suggests this dual targeting approach is sufficient to induce cell death
275 across different AML subtypes even in the presence of extrinsic factor support from MSCs. Further
276 analysis also showed that combining MP-A08 and venetoclax reduced colony forming units in
277 primary AML patient cells (Supp Figure 13b). Notably, however, even high concentrations of MP-
278 A08 and venetoclax had minimal effects on CD34+ hematopoietic stem/progenitor cells isolated from
279 healthy volunteers (Figure 6f; Supp Figure 13c).

280 We next assessed the efficacy of MP-A08 and venetoclax in vivo using primary AML patient
281 xenografts in NSG mice. Immunohistochemical staining for human leukemic cells in the sternum
282 confirmed systemic orthotopic engraftment in two separate sets of primary AML patient xenografts
283 (Figure 6g). Mice with established disease were treated daily with MP-A08 (100mg/kg), venetoclax

284 (75mg/kg) or the combination for two weeks. This combinational approach significantly reduced the
285 leukemic engraftment compared with the respective monotherapies, as assessed by flow cytometric
286 analysis of hCD45⁺ cells in the bone marrow of these mice (Figure 6h-i). Notably, similar dual
287 therapy with MP-A08 and venetoclax daily for two weeks in control C57Bl/6 mice showed no
288 obvious toxicity, with no deleterious effects on body weight, major bone marrow lineages or blood
289 cell counts (Supp Figure 14).

290 Since MP-A08 enhanced venetoclax-induced killing of AML cells, we sought to expand this
291 finding by identifying venetoclax-resistant patients using the Beat AML Master Trial data (ex vivo
292 drug sensitivity analysis with 122 drugs on 409 patient samples) to assess whether these patients could
293 be resensitised to venetoclax⁴⁶. In addition to the TP53^{mut} cohort identified in the phase II studies of
294 venetoclax with cytarabine or hypomethylating agents^{6,47} we identified patients with *KRAS*, *PTPN11*
295 and *SF3B1* mutations as resistant to venetoclax treatment (Figure 6j), consistent with previous
296 findings⁴⁰. Combined MP-A08 and venetoclax treatment exhibited synergistic anti-AML activity in
297 diagnostic patient samples containing either *PTPN11* or *TP53* mutations (Supp. Table 1, Figure 6k-l)
298 with little effect in patient cells containing a *KRAS* mutation (Figure 6m). Although only from single
299 patients with each mutation, collectively, this data begins to provide pre-clinical evidence for
300 combination therapy with SPHK1 inhibitors to augment the efficacy of venetoclax in a variety of
301 AML subtypes.

302

303 **Discussion**

304 The success of the Bcl-2 inhibitor venetoclax in CLL has revolutionised the therapeutic landscape.
305 Yet, in AML which relies on Mcl-1 for survival,⁷ the modest single agent activity of venetoclax has
306 fuelled the search for new therapies that can be combined with this drug.⁴ In this study, we found that
307 enhancing ceramide accumulation, through targeting SPHK1, may be such an approach with ceramide
308 directly activating PKR, inducing ATF4-mediated transcriptional upregulation of Noxa, a known
309 inducer of Mcl-1 degradation, and acts synergistically with venetoclax to induce apoptosis in AML
310 cells. This synergy extended to both primary AML blasts and iLSCs, suggesting this combinational
311 approach may reduce relapse rates by depleting leukemia-initiating cells. Importantly, this approach

312 also reduced disease engraftment in orthotopic AML patient xenograft models, providing pre-clinical
313 evidence of the targeting of SPHK1 and Bcl-2 as a valid combinational therapy approach in AML.

314 The Beat AML master trial is a multi-centre clinical trial integrating genomics data with in
315 vitro responses to both clinical and pre-clinical agents.⁴⁶ Using this data, we identified patients with a
316 number of mutations including those in *KRAS*, *PTPN11* and *SF3B1* to confer venetoclax resistance in
317 addition to the TP53^{Mut} cohort observed in a phase II study examining cytarabine and venetoclax.⁶
318 Excitingly, SPHK1 inhibition combined with venetoclax was effective in patient samples containing
319 *PTPN11* or *TP53* mutations (Figure 5j,k). The absence of any effect observed in a *KRAS* mutant case
320 may be related to the protective effects of *KRAS* in activating the IRE1 pathway to promote survival,
321 as observed in HSCs.⁴⁸ Follow up analysis with cells from further *KRAS* mutant AML patients is
322 clearly required to confirm if these apparent protective effects of mutant *KRAS* against
323 venetoclax/SPHK1 inhibition holds true. Notably, our analysis suggests AML with *NRAS* mutations,
324 which are more common,⁴⁹ remain sensitive to combination therapy with venetoclax/SPHK1
325 inhibition, as demonstrated by data from HL-60 and OCI-AML3 cell lines (Figure 5e,g) and patient
326 sample AML11 (Figure 6i). Collectively this suggests that SPHK1 inhibition may be an effective
327 combination therapy approach with venetoclax in cases that are venetoclax insensitive. Since SPHK1
328 inhibition increases Noxa in a manner independent of TP53, its combination with drugs like
329 cytarabine that are ineffective in cohorts such as TP53^{Mut} patients, may also be warranted.

330 Approaches to enhance cellular ceramide as a potential anti-AML therapy have been
331 investigated over the last two decades,¹⁰ including with inhibitors of SPHK1^{12,13,50} and acid
332 ceramidase,^{51,52} and more recently with direct nanoliposomal ceramide formulations.^{53,54} The
333 mechanisms whereby ceramide elicits its anti-AML effects, however, have not been clear. In this
334 study we showed that accumulation of ceramides through SPHK1 inhibition activates an apoptotic
335 ISR that is dependent on PKR. Although ISR activation has been reported previously in response to
336 addition of exogenous ceramides,⁵⁵ this is the first time to our knowledge that endogenous ceramides
337 have been associated with ISR activation, and the first report of direct activation of PKR by
338 ceramides. Furthermore, we have provided evidence that Noxa is a significant effector of the
339 apoptotic effects of ceramide accumulation through the ISR, expanding the role of sphingolipids in

340 dictating cell survival. This builds on previous studies suggesting ceramide may act both prior to
341 apoptosis through Bcl-2 dephosphorylation⁵⁶ and Bad activation,⁵⁷ as well as during apoptosis through
342 the formation of ceramide-induced channels in the mitochondrial outer membrane to facilitate release
343 of cytochrome c and other pro-apoptotic mediators.⁵⁸

344 Notably, an oncogenic role for PKR in AML has been previously reported, with high PKR
345 expression in AML associated with poor patient prognosis. This appears to be due to the suppressive
346 effects of PKR on the DNA damage response (DDR), an important feature of efficacy to
347 chemotherapeutics such as cytarabine and daunorubicin.⁵⁹ Thus, these observations, combined with
348 the findings of the current study that show that the anti-AML effects of SPHK1 inhibition appear to be
349 independent of TP53 and DDR activation and dependent on PKR activation, make it tempting to
350 speculate that high PKR expressing patients may respond better to SPHK1 inhibition than to
351 chemotherapy.

352 Our findings support a prominent role for the PKR/ATF4/Noxa/Mcl-1 axis identified in this
353 study in mediating ceramide-induced AML cell death. However, efficient Noxa knockdown does not
354 completely rescue AML cell killing by MP-A08 (Figure 1f), supporting the notion that other pathways
355 may play minor roles in the anti-AML effects of MP-A08. Our analysis of gene expression changes in
356 AML cells in response to MP-A08¹² suggest a range of altered pathways that could potentially be
357 involved, including oxidative stress and autophagy, as well as other target genes downstream of ATF4
358 and one of its effectors, CHOP (Supp Table 2). This warrants further investigation.

359 Recent work has revealed an importance for ATF4, the master regulator of the ISR, in
360 leukemic survival.^{60,61} In particular, ATF4 has been shown to promote cell survival in FLT3-ITD⁺
361 AML by enhancing autophagy.⁶² Others have shown that primitive leukemic stem cells (LSCs) exhibit
362 higher basal ISR activity and ATF4 levels than leukemic progenitors/blasts and this may protect LSCs
363 against amino acid deprivation.⁶⁰ Yet, we and others have found that ATF4 can prime cancer cells for
364 apoptosis via transcriptional upregulation of Noxa.^{20,63} How LSCs control the dichotomous signaling
365 of ATF4 to favour survival signaling and how ceramide disrupts this requires further investigation. As
366 ATF4 is regulated by phosphorylation,⁶⁴ we cannot discount the premise that ceramide, a known
367 activator of protein phosphatases, including PP2A,⁶⁵ may also modulate ATF4 at the post-translational

368 level. Indeed, a recent study demonstrated that PP2A activation caused upregulation of ATF4 and
369 Noxa, strengthening the potential link between ceramide and the ISR.⁶⁶ Furthermore, ceramides
370 induce loss of oxidative phosphorylation, a metabolic vulnerability of quiescent LSPCs.^{67,68}
371 Collectively this suggests that ceramide inducing agents together with venetoclax may represent a
372 LSC specific therapy by activating the ISR, reducing the likelihood of relapse and chemotherapy
373 resistant disease (Figure 7).

374

375

376 **Acknowledgements**

377 This work was supported by a Research Training Program Scholarship and Royal Adelaide Hospital
378 Dawes Top-up scholarship (to ACL), the Fay Fuller Foundation, the Royal Adelaide Hospital
379 Research Fund, The Hospital Research Foundation, a Senior Research Fellowship (GNT1156693 to
380 SMP), an Early Career Fellowship (PG101400 to TMN) and project grants (GNT1145139 and
381 GNT1184485) from the National Health and Medical Research Council of Australia. DT is supported
382 by Leukemia & Lymphoma Translation Research Program and CSL Centenary Fellowship. The
383 authors are grateful to the South Australian Cancer Research Biobank (SACRB) and the patients who
384 donated samples. We thank Sarah Tamang for technical assistance.

385

386 **Author contributions**

387 ACL, MNT, VSP, ML, GON, TMN, CWB, PABM, DA, DJC, MC, SRA, CT-P, BKD, AGB, MRP,
388 BLG and JAP performed experiments. PGE, GJG and NR provided intellectual input and/or reagents.
389 DMR, ALB and RJD provided patient material and clinical notes. ACL, JAP, DT and SMP designed
390 the studies and analysed the data. ACL, JAP and SMP wrote the manuscript, which all authors
391 critically reviewed and edited.

392

393 **Conflict of interest**

394 The authors declare no relevant conflicts of interest.

395

- 397 1. Albert MC, Brinkmann K, Kashkar H. Noxa and cancer therapy: Tuning up the mitochondrial
398 death machinery in response to chemotherapy. *Mol Cell Oncol.* 2014;1(1):e29906.
- 399 2. Morsi RZ, Hage-Sleiman R, Kobeissy H, Dbaibo G. Noxa: Role in Cancer Pathogenesis and
400 Treatment. *Curr Cancer Drug Targets.* 2018;18(10):914-928.
- 401 3. Roberts AW, Davids MS, Pagel JM, et al. Targeting BCL2 with Venetoclax in Relapsed
402 Chronic Lymphocytic Leukemia. *N Engl J Med.* 2016;374(4):311-322.
- 403 4. Konopleva M, Pollyea DA, Potluri J, et al. Efficacy and Biological Correlates of Response in
404 a Phase II Study of Venetoclax Monotherapy in Patients with Acute Myelogenous Leukemia. *Cancer*
405 *Discovery.* 2016.
- 406 5. Wei AH, Montesinos P, Ivanov V, et al. Venetoclax plus LDAC for newly diagnosed AML
407 ineligible for intensive chemotherapy: a phase 3 randomized placebo-controlled trial. *Blood.*
408 2020;135(24):2137-2145.
- 409 6. DiNardo CD, Tiong IS, Quaglieri A, et al. Molecular patterns of response and treatment
410 failure after frontline venetoclax combinations in older patients with AML. *Blood.* 2020;135(11):791-
411 803.
- 412 7. Glaser SP, Lee EF, Trounson E, et al. Anti-apoptotic Mcl-1 is essential for the development
413 and sustained growth of acute myeloid leukemia. *Genes Dev.* 2012;26(2):120-125.
- 414 8. van Delft MF, Wei AH, Mason KD, et al. The BH3 mimetic ABT-737 targets selective Bcl-2
415 proteins and efficiently induces apoptosis via Bak/Bax if Mcl-1 is neutralized. *Cancer Cell.*
416 2006;10(5):389-399.
- 417 9. Newton J, Lima S, Maceyka M, Spiegel S. Revisiting the sphingolipid rheostat: Evolving
418 concepts in cancer therapy. *Exp Cell Res.* 2015;333(2):195-200.
- 419 10. Lewis AC, Wallington-Beddoe CT, Powell JA, Pitson SM. Targeting sphingolipid
420 metabolism as an approach for combination therapies in haematological malignancies. *Cell Death*
421 *Discovery.* 2018;4(1):72.
- 422 11. Pitson SM. Regulation of sphingosine kinase and sphingolipid signaling. *Trends Biochem Sci.*
423 2011;36(2):97-107.
- 424 12. Powell JA, Lewis AC, Zhu W, et al. Targeting sphingosine kinase 1 induces MCL1-
425 dependent cell death in acute myeloid leukemia. *Blood.* 2017;129(6):771-782.
- 426 13. Paugh SW, Paugh BS, Rahmani M, et al. A selective sphingosine kinase 1 inhibitor integrates
427 multiple molecular therapeutic targets in human leukemia. *Blood.* 2008;112(4):1382-1391.
- 428 14. Dick TE, Hengst JA, Fox TE, et al. The apoptotic mechanism of action of the sphingosine
429 kinase 1 selective inhibitor SKI-178 in human acute myeloid leukemia cell lines. *J Pharmacol Exp*
430 *Ther.* 2015;352(3):494-508.
- 431 15. Hengst JA, Dick TE, Sharma A, et al. SKI-178: A Multitargeted Inhibitor of Sphingosine
432 Kinase and Microtubule Dynamics Demonstrating Therapeutic Efficacy in Acute Myeloid Leukemia
433 Models. *Cancer Transl Med.* 2017;3(4):109-121.
- 434 16. Hengst JA, Hegde S, Paulson RF, Yun JK. Development of SKI-349, a dual-targeted inhibitor
435 of sphingosine kinase and microtubule polymerization. *Bioorg Med Chem Lett.* 2020;30(20):127453.
- 436 17. Czabotar PE, Lee EF, van Delft MF, et al. Structural insights into the degradation of Mcl-1
437 induced by BH3 domains. *Proc Natl Acad Sci U S A.* 2007;104(15):6217-6222.
- 438 18. Oda K, Arakawa H, Tanaka T, et al. p53AIP1, a potential mediator of p53-dependent
439 apoptosis, and its regulation by Ser-46-phosphorylated p53. *Cell.* 2000;102(6):849-862.
- 440 19. Puthalakath H, O'Reilly LA, Gunn P, et al. ER stress triggers apoptosis by activating BH3-
441 only protein Bim. *Cell.* 2007;129(7):1337-1349.
- 442 20. Wang Q, Mora-Jensen H, Weniger MA, et al. ERAD inhibitors integrate ER stress with an
443 epigenetic mechanism to activate BH3-only protein NOXA in cancer cells. *Proceedings of the*
444 *National Academy of Sciences.* 2009;106(7):2200.
- 445 21. Zyryanova AF, Weis F, Faille A, et al. Binding of ISRIB reveals a regulatory site in the
446 nucleotide exchange factor eIF2B. *Science.* 2018;359(6383):1533.
- 447 22. Bennett MK, Wallington-Beddoe CT, Pitson SM. Sphingolipids and the unfolded protein
448 response. *Biochim Biophys Acta Mol Cell Biol Lipids.* 2019;1864(10):1483-1494.

- 449 23. Bennett MK, Li M, Tea MN, et al. Resensitising proteasome inhibitor-resistant myeloma with
450 sphingosine kinase 2 inhibition. *Neoplasia*. 2022;24(1):1-11.
- 451 24. Halbleib K, Pesek K, Covino R, et al. Activation of the Unfolded Protein Response by Lipid
452 Bilayer Stress. *Molecular Cell*. 2017;67(4):673-684.e678.
- 453 25. Volmer R, Ron D. Lipid-dependent regulation of the unfolded protein response. *Curr Opin*
454 *Cell Biol*. 2015;33:67-73.
- 455 26. Volmer R, van der Ploeg K, Ron D. Membrane lipid saturation activates endoplasmic
456 reticulum unfolded protein response transducers through their transmembrane domains. *Proc Natl*
457 *Acad Sci U S A*. 2013;110(12):4628-4633.
- 458 27. Schnute ME, McReynolds MD, Kasten T, et al. Modulation of cellular S1P levels with a
459 novel, potent and specific inhibitor of sphingosine kinase-1. *Biochem J*. 2012;444(1):79-88.
- 460 28. Draper JM, Xia Z, Smith RA, Zhuang Y, Wang W, Smith CD. Discovery and evaluation of
461 inhibitors of human ceramidase. *Mol Cancer Ther*. 2011;10(11):2052-2061.
- 462 29. Pakos-Zebrucka K, Koryga I, Mnich K, Ljubic M, Samali A, Gorman AM. The integrated
463 stress response. 2016;17(10):1374-1395.
- 464 30. Jammi NV, Whitby LR, Beal PA. Small molecule inhibitors of the RNA-dependent protein
465 kinase. *Biochem Biophys Res Commun*. 2003;308(1):50-57.
- 466 31. Kaufman RJ. Double-stranded RNA-activated protein kinase mediates virus-induced
467 apoptosis: a new role for an old actor. *Proceedings of the National Academy of Sciences of the United*
468 *States of America*. 1999;96(21):11693-11695.
- 469 32. Mukhopadhyay A, Saddoughi SA, Song P, et al. Direct interaction between the inhibitor 2
470 and ceramide via sphingolipid-protein binding is involved in the regulation of protein phosphatase 2A
471 activity and signaling. *FASEB J*. 2009;23(3):751-763.
- 472 33. Heinrich M, Wickel M, Schneider-Brachert W, et al. Cathepsin D targeted by acid
473 sphingomyelinase-derived ceramide. *EMBO J*. 1999;18(19):5252-5263.
- 474 34. Huwiler A, Brunner J, Hummel R, et al. Ceramide-binding and activation defines protein
475 kinase c-Raf as a ceramide-activated protein kinase. *Proc Natl Acad Sci U S A*. 1996;93(14):6959-
476 6963.
- 477 35. Zhang Y, Yao B, Delikat S, et al. Kinase suppressor of Ras is ceramide-activated protein
478 kinase. *Cell*. 1997;89(1):63-72.
- 479 36. Dadsena S, Bockelmann S, Mina JGM, et al. Ceramides bind VDAC2 to trigger
480 mitochondrial apoptosis. *Nat Commun*. 2019;10(1):1832.
- 481 37. Fekry B, Jeffries KA, Esmailniakooshkghazi A, et al. C16-ceramide is a natural regulatory
482 ligand of p53 in cellular stress response. *Nat Commun*. 2018;9(1):4149.
- 483 38. Ewald L, Dittmann J, Vogler M, Fulda S. Side-by-side comparison of BH3-mimetics
484 identifies MCL-1 as a key therapeutic target in AML. *Cell Death Dis*. 2019;10(12):917.
- 485 39. Niu X, Zhao J, Ma J, et al. Binding of Released Bim to Mcl-1 is a Mechanism of Intrinsic
486 Resistance to ABT-199 which can be Overcome by Combination with Daunorubicin or Cytarabine in
487 AML Cells. *Clin Cancer Res*. 2016;22(17):4440-4451.
- 488 40. Phillips DC, Jin S, Gregory GP, et al. A novel CDK9 inhibitor increases the efficacy of
489 venetoclax (ABT-199) in multiple models of hematologic malignancies. *Leukemia*. 2020;34(6):1646-
490 1657.
- 491 41. Ramsey HE, Fischer MA, Lee T, et al. A Novel MCL1 Inhibitor Combined with Venetoclax
492 Rescues Venetoclax-Resistant Acute Myelogenous Leukemia. *Cancer Discov*. 2018;8(12):1566-1581.
- 493 42. Zhang H, Nakauchi Y, Kohnke T, et al. Integrated analysis of patient samples identifies
494 biomarkers for venetoclax efficacy and combination strategies in acute myeloid leukemia. *Nat*
495 *Cancer*. 2020;1(8):826-839.
- 496 43. Ekert PG, Jabbour AM, Manoharan A, et al. Cell death provoked by loss of interleukin-3
497 signaling is independent of Bad, Bim, and PI3 kinase, but depends in part on Puma. *Blood*.
498 2006;108(5):1461-1468.
- 499 44. Chou T-C. Theoretical Basis, Experimental Design, and Computerized Simulation of
500 Synergism and Antagonism in Drug Combination Studies. *Pharmacological reviews*. 2006;58:621-
501 681.

- 502 45. Soderquist RS, Crawford L, Liu E, et al. Systematic mapping of BCL-2 gene dependencies in
503 cancer reveals molecular determinants of BH3 mimetic sensitivity. *Nature Communications*.
504 2018;9(1):3513.
- 505 46. Tyner JW, Tognon CE, Bottomly D, et al. Functional genomic landscape of acute myeloid
506 leukaemia. *Nature*. 2018;562(7728):526-531.
- 507 47. Nechiporuk T, Kurtz SE, Nikolova O, et al. The TP53 Apoptotic Network is a Primary
508 Mediator of Resistance to BCL2 inhibition in AML Cells. *Cancer Discovery*. 2019:CD-19-0125.
- 509 48. Liu L, Zhao M, Jin X, et al. Adaptive endoplasmic reticulum stress signalling via IRE1 α -
510 XBP1 preserves self-renewal of haematopoietic and pre-leukaemic stem cells. *Nature cell biology*.
511 2019;21(3):328-337.
- 512 49. Yu J, Li Y, Li T, et al. Gene mutational analysis by NGS and its clinical significance in
513 patients with myelodysplastic syndrome and acute myeloid leukemia. *Exp Hematol Oncol*. 2020;9:2.
- 514 50. Bonhoure E, Pchejetski D, Aouali N, et al. Overcoming MDR-associated chemoresistance in
515 HL-60 acute myeloid leukemia cells by targeting sphingosine kinase-1. *Leukemia*. 2006;20(1):95-102.
- 516 51. Tan SF, Liu X, Fox TE, et al. Acid ceramidase is upregulated in AML and represents a novel
517 therapeutic target. *Oncotarget*. 2016;7(50):83208-83222.
- 518 52. Pearson JM, Tan SF, Sharma A, et al. Ceramide Analogue SACLAC Modulates Sphingolipid
519 Levels and MCL-1 Splicing to Induce Apoptosis in Acute Myeloid Leukemia. *Mol Cancer Res*.
520 2020;18(3):352-363.
- 521 53. McGill CM, Brown TJ, Fisher LN, et al. Combinatorial Efficacy of Quercetin and
522 Nanoliposomal Ceramide for Acute Myeloid Leukemia. *Int J Biopharm Sci*. 2018;1(1).
- 523 54. Barth BM, Wang W, Toran PT, et al. Sphingolipid metabolism determines the therapeutic
524 efficacy of nanoliposomal ceramide in acute myeloid leukemia. *Blood Adv*. 2019;3(17):2598-2603.
- 525 55. Ruvolo PP, Gao F, Blalock WL, Deng X, May WS. Ceramide regulates protein synthesis by a
526 novel mechanism involving the cellular PKR activator RAX. *J Biol Chem*. 2001;276(15):11754-
527 11758.
- 528 56. Ruvolo PP, Deng X, Ito T, Carr BK, May WS. Ceramide induces Bcl2 dephosphorylation via
529 a mechanism involving mitochondrial PP2A. *J Biol Chem*. 1999;274(29):20296-20300.
- 530 57. Basu S, Bayoumy S, Zhang Y, Lozano J, Kolesnick R. BAD enables ceramide to signal
531 apoptosis via Ras and Raf-1. *J Biol Chem*. 1998;273(46):30419-30426.
- 532 58. Chang KT, Anishkin A, Patwardhan GA, Beverly LJ, Siskind LJ, Colombini M. Ceramide
533 channels: destabilization by Bcl-xL and role in apoptosis. *Biochim Biophys Acta*. 2015;1848(10 Pt
534 A):2374-2384.
- 535 59. Cheng X, Byrne M, Brown KD, et al. PKR inhibits the DNA damage response, and is
536 associated with poor survival in AML and accelerated leukemia in NHD13 mice. *Blood*.
537 2015;126(13):1585-1594.
- 538 60. van Galen P, Mbong N, Kreso A, et al. Integrated Stress Response Activity Marks Stem Cells
539 in Normal Hematopoiesis and Leukemia. *Cell Rep*. 2018;25(5):1109-1117.e1105.
- 540 61. Zhou C, Martinez E, Di Marcantonio D, et al. JUN is a key transcriptional regulator of the
541 unfolded protein response in acute myeloid leukemia. *Leukemia*. 2017;31(5):1196-1205.
- 542 62. Heydt Q, Larrue C, Saland E, et al. Oncogenic FLT3-ITD supports autophagy via ATF4 in
543 acute myeloid leukemia. *Oncogene*. 2018;37(6):787-797.
- 544 63. Armstrong JL, Flockhart R, Veal GJ, Lovat PE, Redfern CP. Regulation of endoplasmic
545 reticulum stress-induced cell death by ATF4 in neuroectodermal tumor cells. *J Biol Chem*.
546 2010;285(9):6091-6100.
- 547 64. Sharma K, D'Souza RC, Tyanova S, et al. Ultradeep human phosphoproteome reveals a
548 distinct regulatory nature of Tyr and Ser/Thr-based signaling. *Cell Rep*. 2014;8(5):1583-1594.
- 549 65. Chalfant CE, Kishikawa K, Mumby MC, Kamibayashi C, Bielawska A, Hannun YA. Long
550 chain ceramides activate protein phosphatase-1 and protein phosphatase-2A. Activation is
551 stereospecific and regulated by phosphatidic acid. *J Biol Chem*. 1999;274(29):20313-20317.
- 552 66. Ryder CB, Narla G. Direct-Acting Small Molecule Activators of PP2A (SMAPs) in Myeloid
553 Malignancies: Understanding Mechanisms of Cytotoxicity to Inform Rational Combinatorial
554 Therapeutic Strategies. *Blood*. 2017;130(Supplement 1):2517-2517.
- 555 67. Morad SAF, Ryan TE, Neuffer PD, et al. Ceramide-tamoxifen regimen targets bioenergetic
556 elements in acute myelogenous leukemia. *Journal of lipid research*. 2016;57(7):1231-1242.

557 68. Lagadinou ED, Sach A, Callahan K, et al. BCL-2 inhibition targets oxidative phosphorylation
558 and selectively eradicates quiescent human leukemia stem cells. *Cell stem cell*. 2013;12(3):329-341.
559

560 **Figure Legends**

561 **Figure 1: BH3 only proteins Noxa and Bim are essential for MP-A08 induced cell death**

562 **A)** Mcl-1 immunoprecipitation of MV411 cells treated with MP-A08 for 6 h and subjected to
563 immunoblot analysis with the indicated antibodies. **B)** Quantitative PCR analysis of MV411 cells
564 treated with MP-A08 (20 μ M) over 6 h. **C)** Immunoblot analysis of MV411 cells treated with MP-A08
565 in the presence of cycloheximide for 6 h. **D)** MV411 or **E)** OCI-AML3 were treated with increasing
566 concentrations of MP-A08 for 6 h and subject to immunoblot analysis with the indicated antibodies.
567 MV411 cells were lentivirally transduced with shRNAs targeting **F)** Noxa, **G)** Bim or **H)** Bid, treated
568 with doxycycline for 48 h and MP-A08 (15 μ M) for either 6 h for immunoblot analysis or 24 h for cell
569 viability using Annexin V staining. All qualitative data is representative of at least three independent
570 experiments, and all quantitative data shown represents mean \pm SEM from three independent
571 experiments. Statistical significance was assessed by Student's t test. *** $p < 0.0001$, ** $p < 0.005$, *
572 $p < 0.05$.

573

574 **Figure 2: MP-A08 induces ATF4 dependent Noxa transcription**

575 **A)** MV411 cells were treated with MP-A08 (20 μ M), daunorubicin (DNR) (1 μ M) or cytarabine (Ara-
576 **C)** (1 μ M) for 6 h, lysed and subject to immunoblot analysis with indicated antibodies. **B)** Schematic
577 of the unfolded protein response. **C)** MV411 cells were treated with MP-A08 (20 μ M) over a 6 h
578 period, lysed and subject to immunoblot analysis with the indicated antibodies. **D)** MV411 cells were
579 stably transduced with a two different CRISPR guide sequences targeting SPHK1 (g1 and g2) and
580 lysed and subject to immunoblot analysis with indicated antibodies. SPHK1 knockout efficiency was
581 confirmed via SPHK1 activity assays of lysates from these cells using assay conditions largely
582 selective for SPHK1 over SPHK2 (Supp. Figure 5c). **E)** MV411 cells were treated with MP-A08
583 (20 μ M) alone or in combination with eIF2b agonist, ISRIB (200nM) over 6 h for quantitative PCR
584 analysis of Noxa mRNA levels and immunoblot analysis with the indicated antibodies. Statistical
585 significance was assessed by Student's t test. * $p < 0.05$ (n=3). **F)** MV411 cells were stably transduced

586 with a doxycycline inducible shRNA targeting ATF4. Cells were treated with 1µg/ml doxycycline for
587 48 h and MP-A08 (20µM) for 6 h prior to cell lysis for immunoblot analysis. ns denotes non-specific
588 band. **G)** Chromatin immunoprecipitation analysis of the Noxa promoter in response to MP-A08
589 treatment (20µM) of MV411 cells for 6 h. Statistical significance was assessed by Student's t test. *
590 $p < 0.05$ (n=4). **H)** Primary AML samples were treated with increasing concentrations of MP-A08 and
591 subject to immunoblot analysis with the indicated antibodies. All qualitative data is representative of
592 at least three independent experiments, and all quantitative data shown represents mean \pm SEM from at
593 least three independent experiments.

594

595 **Figure 3: Ceramides drive a PERK-independent ISR**

596 **A-C)** MV411 cells were treated with vehicle control (0.1% DMSO; black bars) or 20µM MP-A08
597 (red bars) for 6 h and analysed by LC-MS. **A)** Quantitation of individual ceramide (Cer) and
598 dihydroceramide (dhCer) species. **B)** Quantitation of sphingosine (Sph) and dihydrosphingosine
599 (dhSph) species. **C)** Quantitation of sphingosine 1-phosphate (S1P) and dihydrosphingosine 1-
600 phosphate (dhS1P). All data are presented as pmol per million cells, mean \pm SD from four independent
601 experiments. Statistical significance was assessed by Student's t test. (* $p < 0.05$, ** $p < 0.01$, *** $p <$
602 0.001). **D)** MV411 cells were treated with MP-A08 (20µM), PF-543 (1µM) and SK1-I (10µM) for 6
603 h, lysed and subject to immunoblot analysis. **E)** MV411 cells were treated with Ceranib-2 for 16 h and
604 assessed for cell viability by Annexin V/propidium iodide staining. Data represents mean \pm SD from
605 two independent experiments. MV411 cells were treated with Ceranib-2 (10µM) for 6 h and subject to
606 immunoblot analysis with the indicated antibodies. **F)** MV411 cells were treated with MP-A08
607 (20µM) C2-Ceramide (10µM), C6-Ceramide (10µM), C2-dhCeramide (10µM), C6-dhCeramide
608 (10µM) (all introduced from 2.5mM stock solutions in DMSO), Bortezomib (10nM) for 6 h, lysed
609 and subject to immunoblot analysis with the indicated antibodies. **G)** HAP1 wild type and *PERK*^{-/-}
610 cells were treated with MP-A08 (20µM) for 6 h, lysed and subject to immunoblot analysis with the
611 indicated antibodies. **H,I)** MV411 cells were stably transduced with a doxycycline inducible shRNA
612 targeting PERK. Cells were treated with 1µg/ml doxycycline for 48 h and MP-A08 (20µM) for 6 h

613 prior to (H) quantitative PCR analysis of PERK mRNA levels and (I) immunoblot analysis with the
614 indicated antibodies. Data shown represents mean \pm SEM from three independent experiments.
615 Statistical significance was assessed by Student's t test. ** $p < 0.01$.

616

617 **Figure 4: Ceramides drive a PKR-dependent integrated stress response**

618 **A)** Schematic of the integrated stress response (ISR). **B,C)** MV411 cells, OCI-AML3 cells, MOLM13
619 cells, HL-60 cells and THP-1 cells were treated with MP-A08 alone (20 μ M) or in combination with
620 GCN2 inhibitor A-92 (5 μ M), PKR inhibitors C16 (5 μ M) or 2-AP (0.1-10mM) or PERK inhibitor
621 AMG-44 (5 μ M) for 6 h prior to immunoblot analysis with indicated antibodies. **D)** MV411 cells were
622 treated with MP-A08 (10 μ M), and 2-AP (5mM) for 16 h and assessed for cell viability by Annexin
623 V/propidium iodide staining. Data shown represents mean \pm SEM from three independent
624 experiments. Statistical significance was assessed by Student's t test. **E)** WT or PKR knockout
625 MV411 cells were treated with MP-A08 (15 μ M) for 16 h and assessed for cell viability by Annexin
626 V/ propidium iodide staining. Data shown represents mean \pm SEM from four independent
627 experiments. Statistical significance was assessed by Student's t test. Immunoblot analysis of WT or
628 PKR knockout MV411 cells with the indicated antibodies. **F)** PKR-HA was immunoprecipitated from
629 transiently transfected HEK 293T cells, incubated with exogenous C6-ceramide (10 μ M) for 30 mins
630 and subjected to a PKR activity assay, using auto-phosphorylation as the read-out. Data shown
631 represents mean \pm SEM from four independent experiments. **G)** Lysates from HEK293T cells
632 transfected with pcDNA3/PKR-HA was incubated with ceramide conjugated to agarose beads or
633 control beads overnight at 4°C, washed and resolved by SDS-PAGE and the associated PKR detected
634 by immunoblotting with anti-HA antibodies using an Odyssey imaging system.

635

636 **Figure 5: MP-A08 and venetoclax induces potent synergistic activity in AML cell lines**

637 **A)** MV411 cells were treated with 20 μ M MP-A08 (black bars), 10nM venetoclax (red bars) alone or
638 in combination (white bars) for up to 6 h. Cell viability was analysed every 2 h by Annexin
639 V/propidium iodide staining. Data is representative of mean \pm SEM (n=4). Statistical significance was

640 assessed by Student's t test. (**** $p < 0.0001$). Drug synergy was assessed using the Chou-Talay
641 combination Index (CI) method whereby CI values less than 1 are classified as synergy. **B)** FDM wild
642 type and Bax/Bak^{-/-} cells treated with MP-A08 (20 μ M) and/or venetoclax (10nM). Data is
643 representative of mean \pm SEM (n=4). Statistical significance was assessed by Student's t test. (**** p
644 < 0.0001). **C,D)** MV411, **E)** HL-60 **F)** MOLM13 **G)** OCI-AML3. **H)** MV411 cells were stably
645 transduced with a doxycycline inducible shRNA targeting Bcl-2 and treated with doxycycline
646 (1 μ g/ml) for 48 h and MP-A08 (10 μ M) for 24 h. Cell viability was assessed by Annexin V staining.
647 All data represents mean \pm SEM from three independent experiments. Statistical significance was
648 assessed by Student's t test. *** $p < 0.0001$. **I)** UT-7 cells were treated with MP-A08 and venetoclax
649 for 24 h and assessed for cell viability by Annexin V/propidium iodide staining. Drug synergy was
650 assessed using the Chou-Talay combination Index (CI) method whereby CI values less than 1 are
651 classified as synergy. **J)** UT-7 were treated with increasing concentrations of MP-A08 for 6 h and
652 subject to immunoblot analysis. **K)** MV411 and **L)** OCI-AML3 cells were treated with MP-A08,
653 venetoclax or in combination for 6 h and subject to immunoblot analysis with the indicated
654 antibodies. All qualitative data is representative of at least three independent experiments, and all
655 quantitative data shown represents mean \pm SEM from at least three independent experiments.

656

657 **Figure 6: MP-A08 and venetoclax treatment exhibits anti-leukemic activity in primary AML**

658 *samples*

659 **A)** Primary AML cells were treated with increasing concentrations of MP-A08 for 6 h, lysed and
660 subject to immunoblot analysis with indicated antibodies. **B,C)** Primary AML samples were treated
661 with MP-A08 and venetoclax for 6 h and assessed for cell viability by Annexin V staining. Data is
662 displayed as duplicate technical replicates mean \pm range Statistical significance was assessed by
663 Student's t test. (* $p < 0.05$, *** $p < 0.0005$). Synergy was determined by the CI method. **D)** FACS
664 purified iLSCs were seeded alone or **E)** on a MSC co-culture layer, treated with MP-A08 and
665 venetoclax for 24 h and assessed for cell viability by Annexin V staining. Data is displayed as

666 duplicate technical replicates mean \pm range. Statistical significance was assessed by Student's t test.
667 (* $p < 0.05$). Synergy was determined by the Webb fractional product (FP) method. **F)** Normal bone
668 marrow derived CD34⁺ cells were treated with MP-A08 and venetoclax for 6 h and assessed for cell
669 viability by Annexin V staining. Data is displayed as duplicate technical replicates mean \pm range. **G)**
670 Representative immunohistochemistry staining using human specific mitochondrial antibody
671 (MTC02) of a NSG mouse sternum engrafted with primary AML cells. Scale bar equals 100 μ M. **H,I)**
672 NSG mice were engrafted with primary AML blasts, and bled weekly to confirm disease engraftment
673 (>1% hCD45⁺ in peripheral blood). Mice were administered with either vehicle, MP-A08 (i.p. 100
674 mg/kg), venetoclax (p.o. 75mg/kg) or both daily for two weeks. Engraftment was quantified by
675 assessing the percentage of human CD45⁺ cells in the bone marrow of recipient mice. Each symbol
676 represents the percentage of CD45⁺ cells observed in a separate mouse. Significance was assessed by
677 Student's t test. **J)** Mutational analysis of AML patient samples treated with venetoclax from the Beat
678 AML Project.⁴⁶ Average area-under-the curve (AUC) is a measure of drug sensitivity (higher the
679 AUC = more resistant) derived from an ex vivo drug sensitivity assays. Statistical significance was
680 assessed by Student's t test with Welch's correction. (** $p < 0.01$, *** $p < 0.0001$). **K)** Primary AML
681 samples identified by whole exome sequencing containing PTPN11, **L)** TP53 or **M)** K-Ras mutations
682 were treated with MP-A08 and venetoclax for 6 h and assessed for cell viability by Annexin V
683 staining. Data is displayed as duplicate technical replicates, mean \pm range. Statistical significance was
684 assessed by Student's t test. (** $p < 0.01$).

685

686 **Figure 7: Ceramides induce ISR activation and sensitises cells to Bcl-2 inhibition**

687 The accumulation of pro-apoptotic sphingolipids such as ceramide in response to SPHK inhibition is
688 sensed by eIF2a kinase PKR. PKR activation culminates in an apoptotic ISR mediated by master
689 transcription factor ATF4. ATF4 promotes Bcl-2 dependency by the transcriptional upregulation of
690 Noxa and the subsequent binding to and inactivation of Mcl-1.

Figure 1: BH3 only proteins Bim and Noxa are essential for MP-A08 induced cell death.

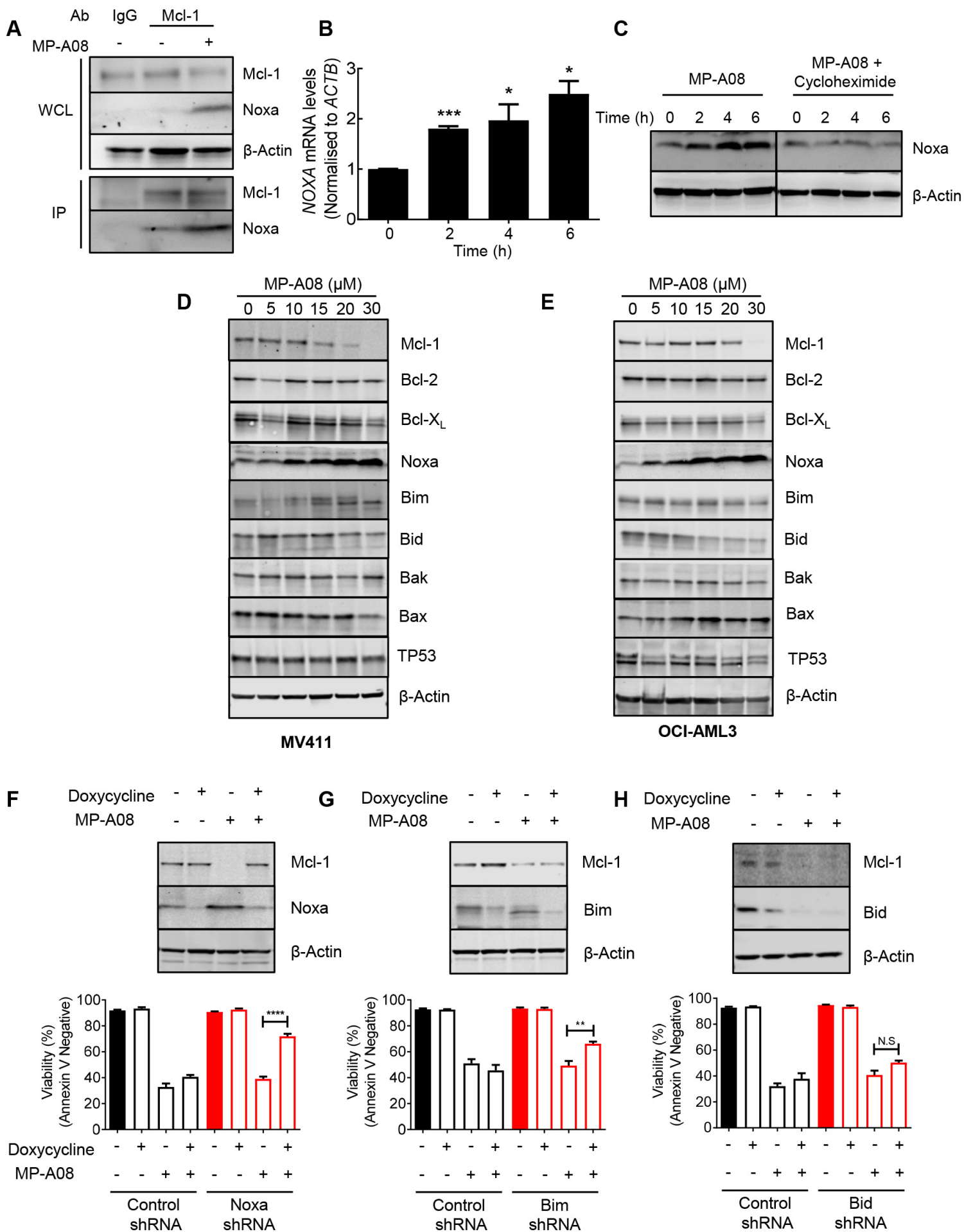


Figure 2: MP-A08 induces ATF4 dependent Noxa transcription

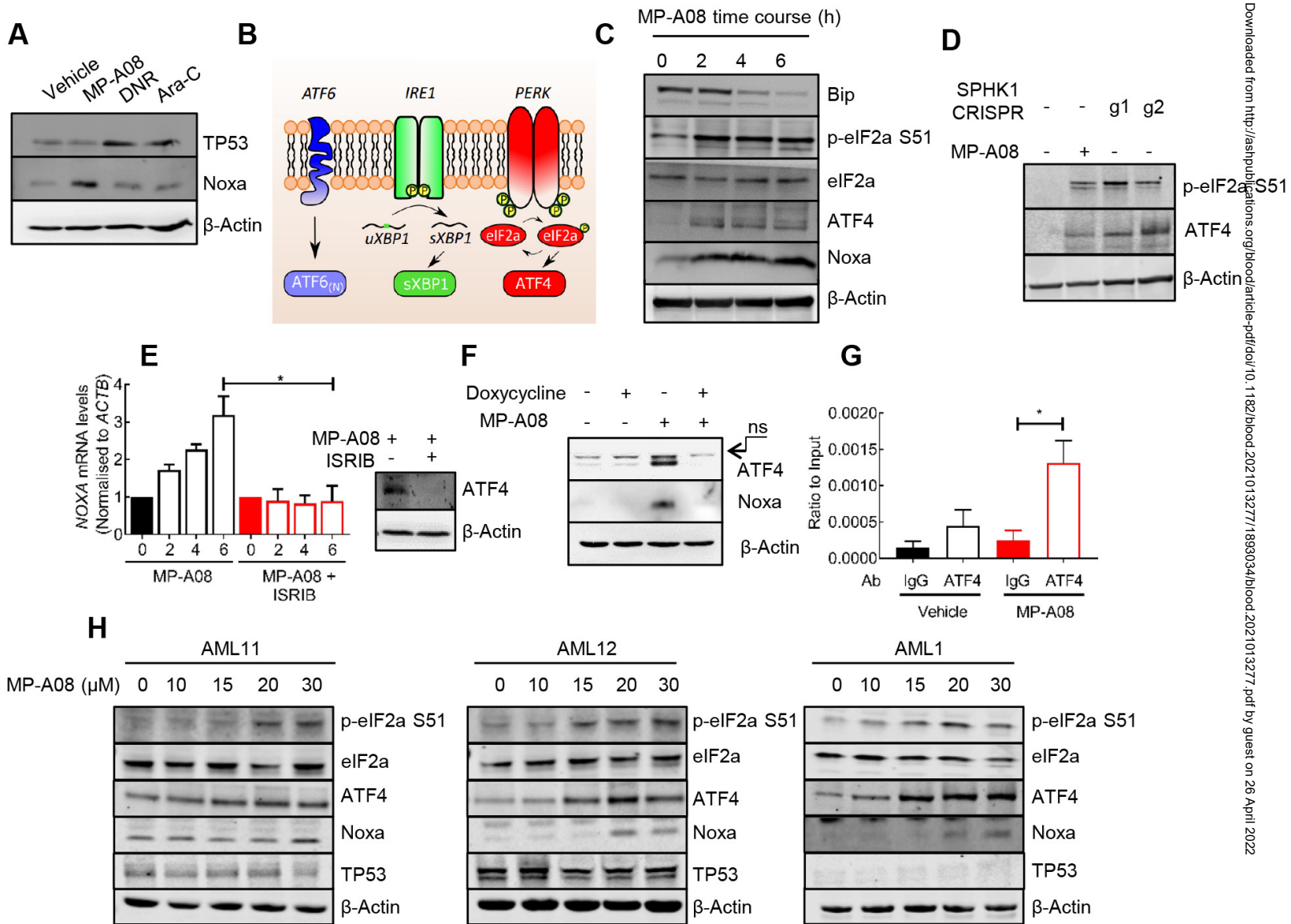


Figure 3: Ceramides drive a PERK-independent ISR

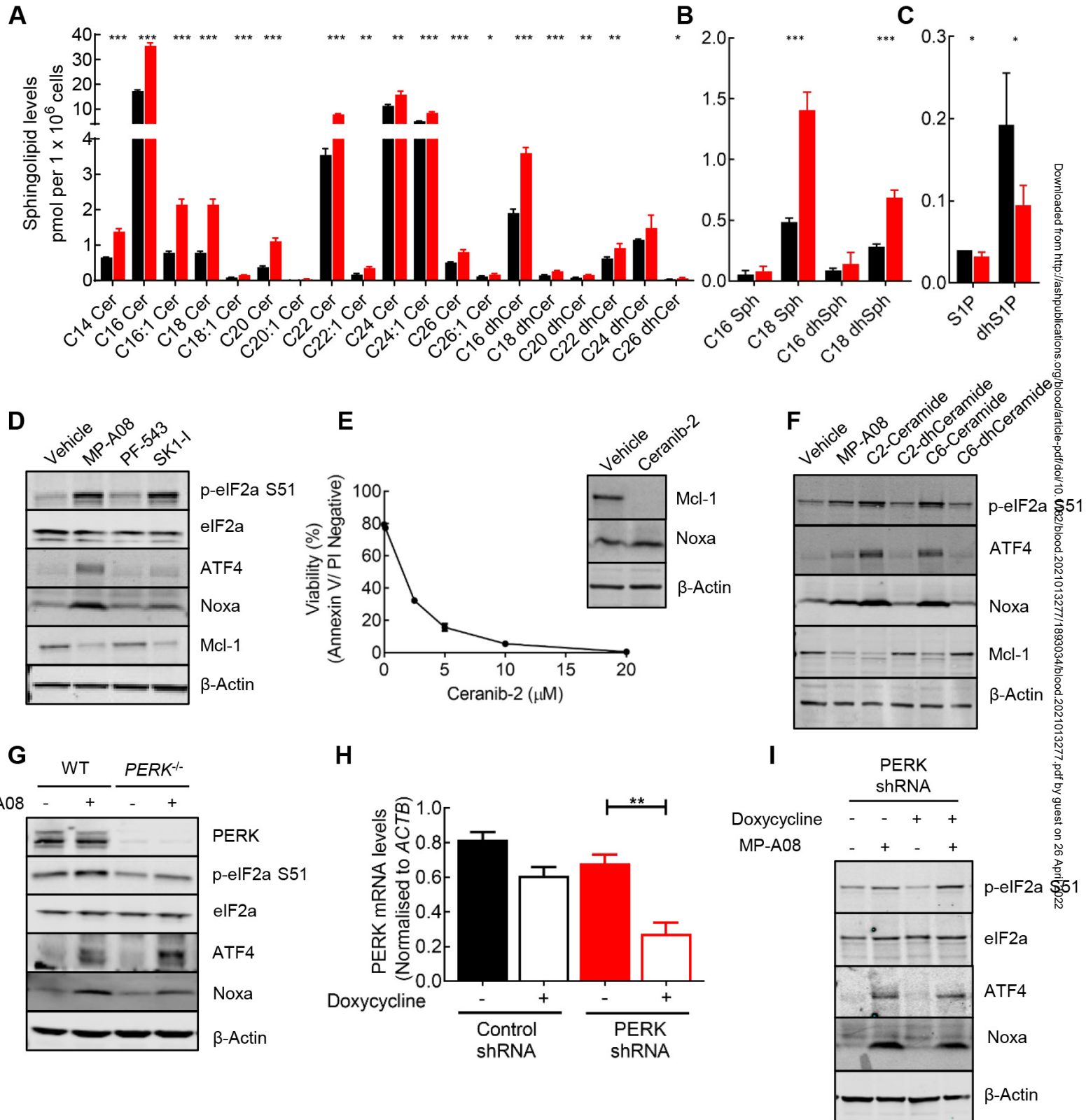


Figure 4: Ceramides drive a PKR-dependant integrated stress response (ISR)

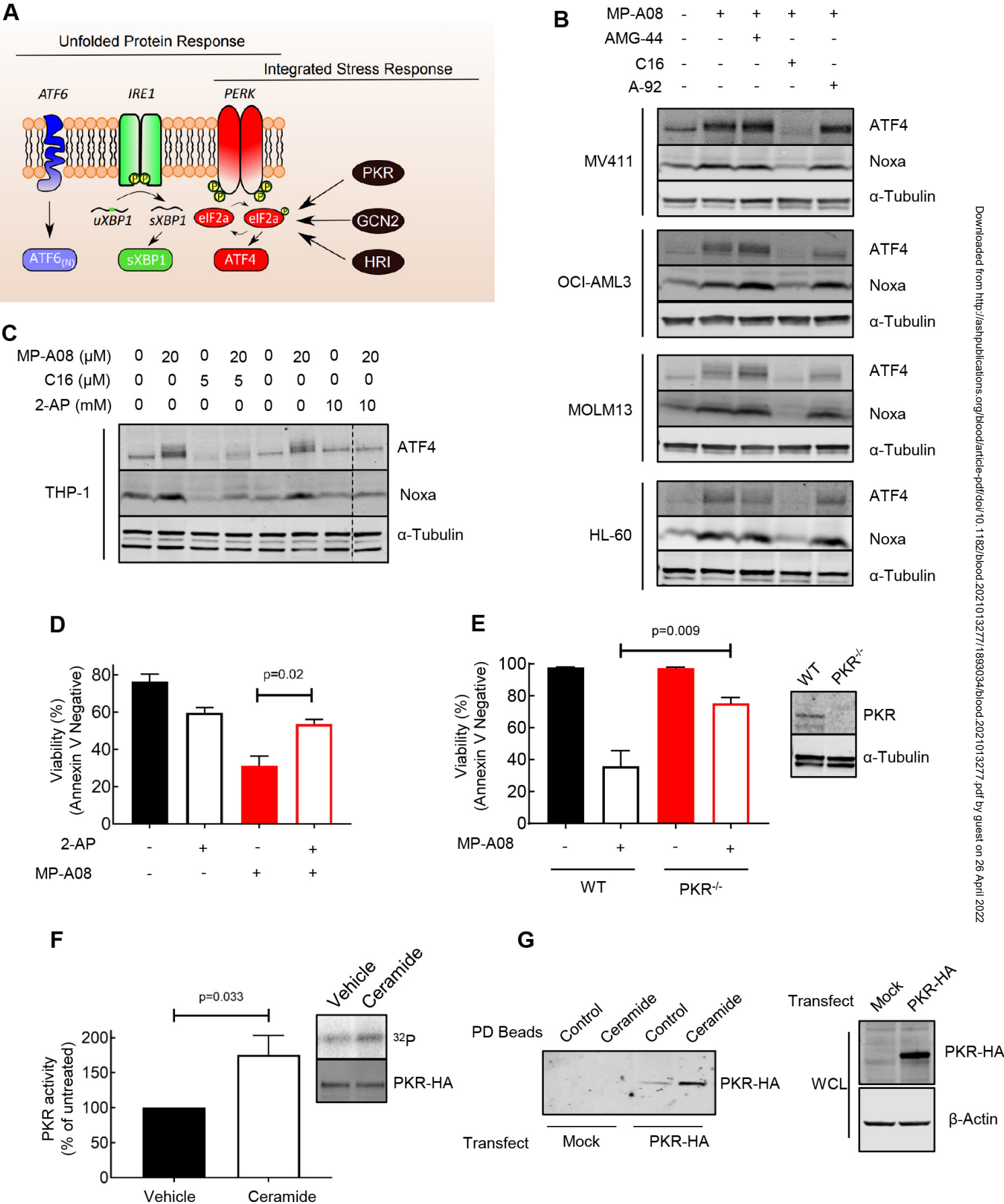


Figure 5: MP-A08 and venetoclax induces potent synergistic activity in AML cell lines

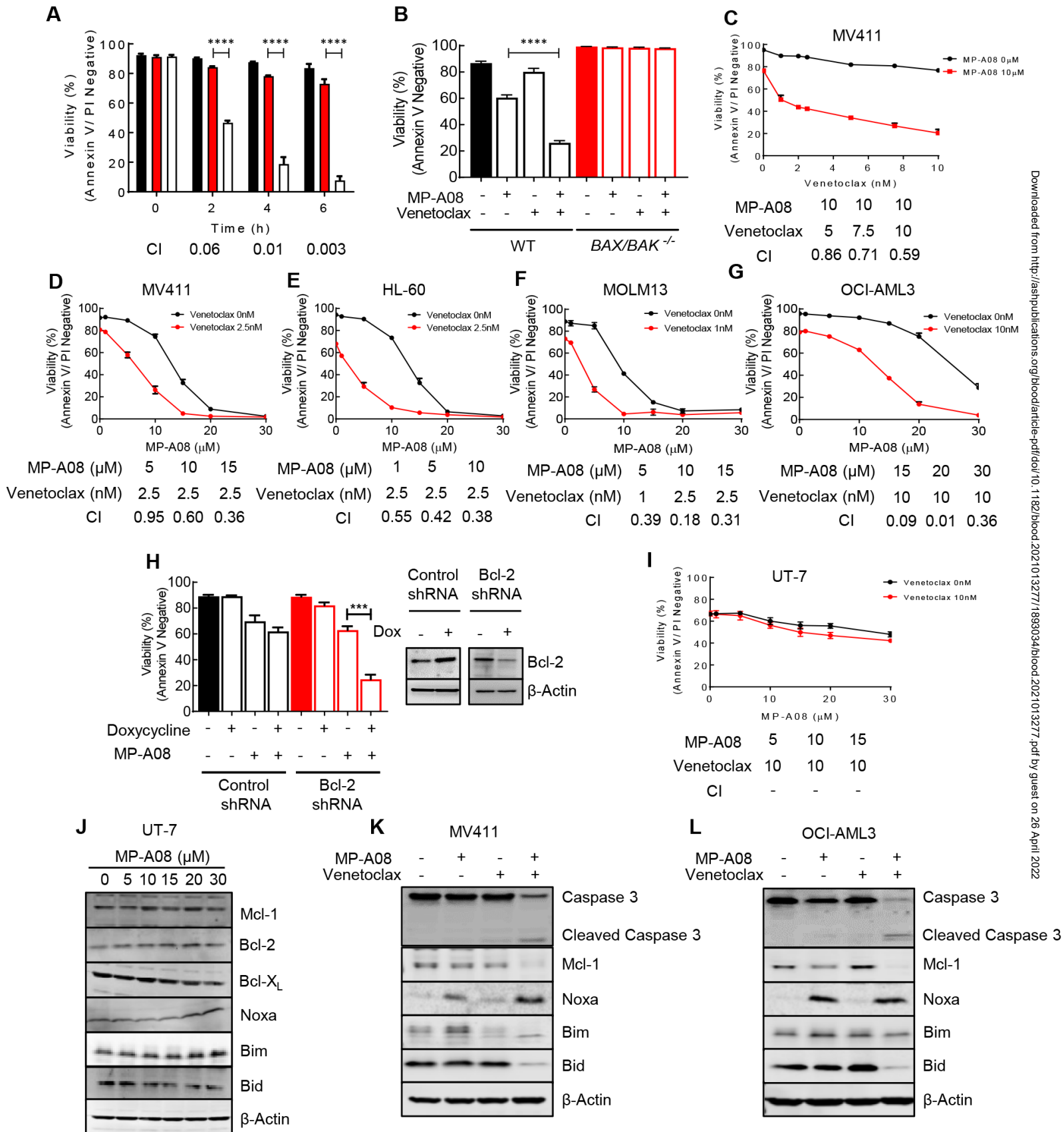


Figure 6: MP-A08 & Venetoclax treatment exhibits anti-leukemic activity in primary AML samples

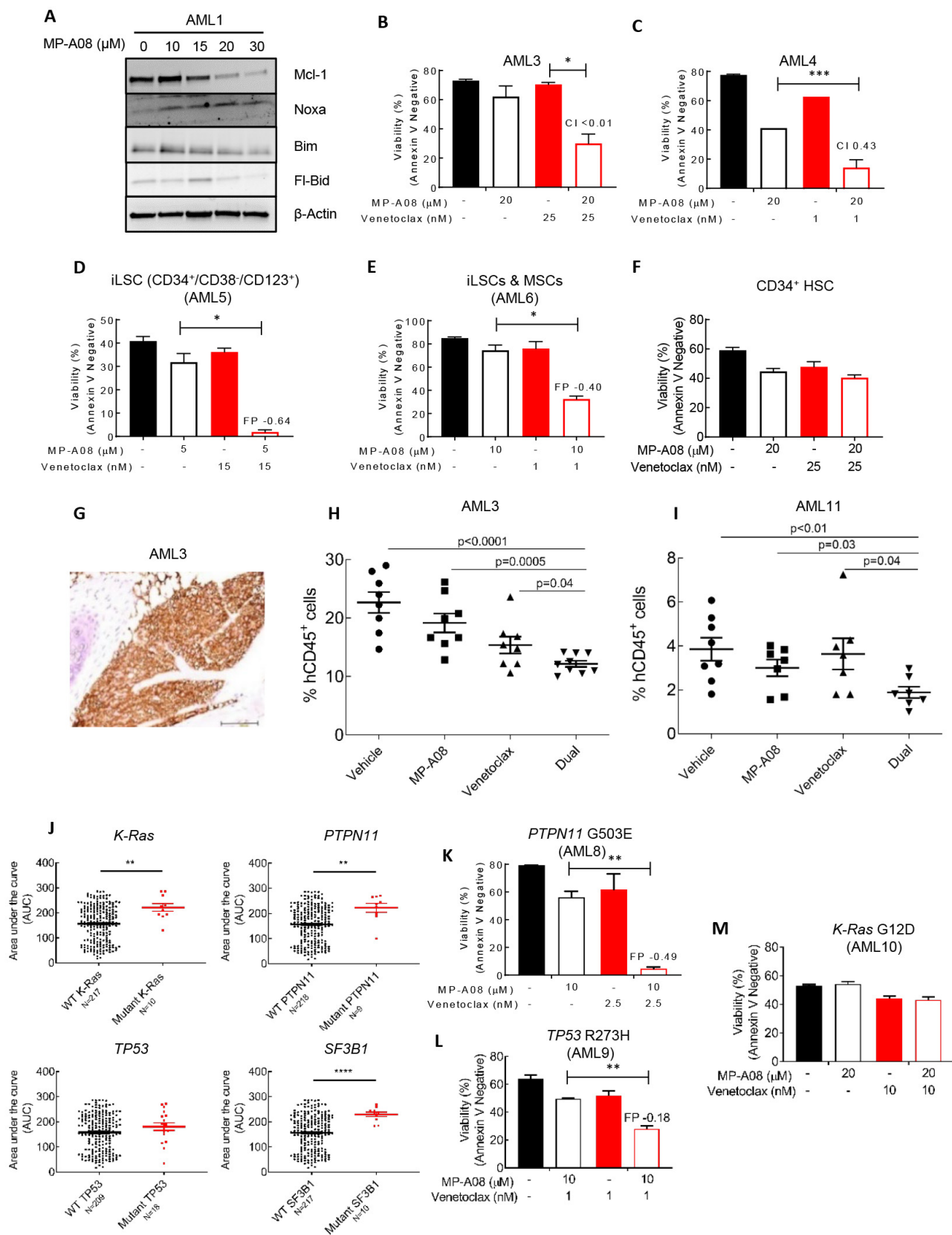


Figure 7: Ceramides induce ISR activation and sensitises cells to Bcl-2 inhibition

